

Forschungszentrum Karlsruhe
Technik und Umwelt

Wissenschaftliche Berichte
FZKA 6701

**ITER ECRF Advanced Source Development
– Coaxial Cavity Gyrotron –**

– Final Report –

ITER Task No.: G 52 TT 22 EU (TWO-ADV/SOR)

B. Piosczyk, A. Arnold, H. Budig, G. Dammertz, O. Drumm,
M. Kuntze, M. Thumm

Institut für Hochleistungsimpuls- und Mikrowellentechnik
Programm Kernfusion
Association EURATOM-FZK

Forschungszentrum Karlsruhe GmbH, Karlsruhe

2002

Impressum der Print-Ausgabe:

**Als Manuskript gedruckt
Für diesen Bericht behalten wir uns alle Rechte vor**

**Forschungszentrum Karlsruhe GmbH
Postfach 3640, 76021 Karlsruhe**

**Mitglied der Hermann von Helmholtz-Gemeinschaft
Deutscher Forschungszentren (HGF)**

ISSN 0947-8620

ITER ECRF ADVANCED SOURCE DEVELOPMENT

- Coaxial Cavity Gyrotron -

- Final Report -

ITER task No.: G 52 TT 22 EU (TWO-ADV/SOR)

Executive Summary:

In accordance with the goal of the ITER task experimental and theoretical investigations on the coaxial cavity gyrotron have been continued. A status has been achieved where a decision about an industrial realization of a 2 MW, CW 170 GHz coaxial cavity gyrotron can be taken. In addition, first work on integration of such a coaxial gyrotron has been done.

The measurements have been performed with an experimental tube constructed in a modular way. The gyrotron has been designed to operate in the $TE_{31,17}$ mode at 165 GHz. The cavity has been optimized for the nominal parameters: cathode voltage $U_c = 90$ kV, beam current $I_b = 50$ A, microwave output power $P_{out} = 1.5$ MW. In general, the measurements have been performed at short pulses (typically 1 ms) with a repetition rate of 1 Hz. However, in order to investigate the behavior at longer pulses, single pulse operation with extended pulse lengths has been examined.

The achievements can be summarized as follows:

- The mechanism of the parasitic low frequency oscillations has been understood and the occurrence of such oscillations have been suppressed successfully.
- Efficient microwave output power generation has been achieved in single mode operation in good agreement with results of numerical simulations. In particular the following experimental results have been obtained:

maximum RF-output power:

$$P_{out} \cong 2.2 \text{ MW} \quad \text{with} \quad U_c \cong 94.6 \text{ kV}, \quad I_b \cong 84 \text{ A}$$

maximum output efficiency η_{out} at $P_{out} \cong 1.5$ MW:

$$\eta_{out} \cong 30 \% \quad \text{with} \quad U_c \cong 90.4 \text{ kV}, \quad I_b \cong 56 \text{ A}$$

$$\eta_{out} \cong 48 \% \quad \text{with} \quad U_{coll} \cong -34 \text{ kV}, \quad \text{with depressed collector}$$

- Stable electron beam current up to 84 A at $U_c \cong 90$ kV and velocity ratio $\alpha \cong 1.4$ has been obtained.
- The microwave pulse length has been extended up to 17 ms, limited due to a type of a Penning discharge in the gun region. The origin of this limitation has been investigated and

found to be related to the possibility of electron trapping within the gun. Possibilities to avoid this limitation are suggested.

- The current to the insert saturates at nominal parameters after a few ms at a value < 30 mA.
- The amplitude of the mechanical vibrations of the insert has been measured to be within ± 0.03 mm caused mainly due to the flow of the cooling water. This value is sufficiently low for stable CW operation of a coaxial gyrotron.
- The losses at the insert have been measured to be about 0.1% of the microwave output power, in reasonable agreement with numerical calculations. The cooling capability of the insert is completely sufficient to remove these losses even for a 2 MW, CW tube.
- The amount of the microwave losses captured inside the gyrotron tube has been found to be fairly large, namely about 11% of the RF output power. The uniform distribution of the captured radiation inside the mirror box, however, reduces the technical problems due to absorption of the stray radiation in the walls of the box. Some reduction of the amount of the stray radiation is expected from a further optimization of the mirrors.
- By biasing the coaxial insert a fast (within ≈ 0.1 ms) frequency tuning has been demonstrated. In particular, a fast step frequency tuning between the 165 GHz nominal mode and the azimuthal neighbors at 162.75 GHz and 167.2 GHz have been performed. In addition, at the nominal mode a continuous frequency variation within the bandwidth of up to 70 MHz have been done.

The different gyrotron components have been investigated for their usability in a 2 MW, CW gyrotron. The $TE_{34,19}$ mode has been selected in agreement with technical restrictions for the 2 MW, 170 GHz coaxial gyrotron. A collector suitable for handling the remaining beam power of 2.4 MW has been suggested and a technical design has been performed in collaboration with TED, Velizy, France.

The obtained results are presented and discussed in detail in this report.

ITER ECRF ENTWICKLUNG VON FORTSCHRITTLICHEN GYROTRONEN

- Gyrotron mit koaxialer Anordnung -

- Abschlußbericht -

ITER task No.: G 52 TT 22 EU (TWO-ADV/SOR)

Kurzfassung:

In Übereinstimmung mit den Zielen des ITER Programmpunktes wurden sowohl experimentelle als auch theoretische Untersuchungen zum koaxialen Gyrotron fortgesetzt. Der erreichte Stand der Entwicklung ermöglicht es, eine Entscheidung über eine technische Realisierung eines 2 MW, 170 GHz koaxialen Gyrotrons, welches im Dauerstrich (CW) betrieben werden kann, zu fällen.

Die Messungen wurden an einer experimentellen Röhre im modularen Aufbau durchgeführt. Das Gyrotron wurde für einen Betrieb in der $TE_{31,17}$ Mode bei 165 GHz entworfen. Der Resonator wurde für die folgenden Parameter optimiert: Kathodenspannung $U_c = 90$ kV, Strahlstrom $I_b = 50$ A, Mikrowellenleistung $P_{out} = 1.5$ MW. Im allgemeinen wurden die Messungen bei kurzen Pulsen (typischerweise 1 ms) mit einer Wiederholrate von 1 Hz durchgeführt. Um jedoch das Verhalten bei längeren Pulsen zu untersuchen, wurde im Betrieb mit Einzelpulsen die Pulslänge verlängert.

Die erzielten Ergebnisse lassen sich wie folgt zusammenfassen:

- Der Mechanismus, der zur Entstehung parasitärer Schwingungen bei niedrigen Frequenzen führt, wurde verstanden und das Auftreten der parasitären Schwingungen wurde erfolgreich unterdrückt.
- Ein hoher Wirkungsgrad bei der Erzeugung der Mikrowellen (HF) wurde in guter Übereinstimmung mit numerischen Rechnungen erreicht. Im einzelnen wurden folgende Ergebnisse erzielt:

maximale RF-Ausgangsleistung:

$$P_{out} \cong 2.2 \text{ MW} \quad \text{mit} \quad U_c \cong 94.6 \text{ kV}, \quad I_b \cong 84 \text{ A}$$

maximaler Wirkungsgrad η_{out} bei $P_{out} \cong 1.5$ MW:

$$\eta_{out} \cong 30 \% \quad \text{mit} \quad U_c \cong 90.4 \text{ kV}, \quad I_b \cong 56 \text{ A}$$

$$\eta_{out} \cong 48 \% \quad \text{mit} \quad U_{coll} \cong -34 \text{ kV}, \quad \text{mit Energierückgewinnung}$$

- Ein stabiler Elektronenstrahl wurde bis zu einem Strom von 84 A bei $U_c \cong 90$ kV mit $\alpha \cong 1.4$ wurde beobachtet.

- Die Länge des Mikrowellenpulses wurde bis 17 ns verlängert, begrenzt durch das Auftreten einer Penning-Entladung im Bereich der Elektronenkanone. Die Ursache der Begrenzung liegt darin, dass im Bereich der Elektronenkanone Fallen für Elektronen existieren, in denen gefangene Elektronen oszillieren können. Möglichkeiten zum Vermeiden dieses Verhaltens wurden aufgezeigt.
- Bei Nominalparametern sättigt der Strom zum Innenleiter bei einem Wert < 30 mA.
- Die Amplitude der mechanischen Schwingungen des Innenleiters bleibt unter Betriebsbedingungen innerhalb ± 0.03 mm. Dieser Wert ist völlig ausreichend für einen stabilen CW-Betrieb. Die mechanischen Schwingungen des Innenleiters werden hauptsächlich durch den Fluß des Kühlwassers verursacht.
- Die Verluste am Innenleiter betragen unter Betriebsbedingungen etwa 0.1% der HF-Ausgangsleistung. Dieser Wert ist in guter Übereinstimmung mit Rechnungen. Bei der gegebenen Kühlmöglichkeit des Innenleiters kann diese Verlustleistung leicht abgeführt werden.
- In Messungen wurde festgestellt, dass der Anteil der Mikrowellenleistung, welcher als Streustrahlung im Gehäuse des Gyrotrons gefangen wird, relativ groß ist, nämlich etwa 11% von der HF-Ausgangsleistung. Die Beobachtung, dass die gefangene Mikrowellenleistung annähernd isotrop im Gyrotrongeäuse verteilt ist, erleichtert die Abführung der in den Wänden absorbierten Leistung. Von einer weiteren Optimierung der Mikrowellenspiegel wird eine Reduzierung der Streustrahlung erwartet.
- Durch das Anlegen einer Spannung an den Innenleiter wurde eine schnelle (≈ 0.1 ns) Frequenzverstimmung durchgeführt. Sowohl eine stufenweise Frequenzvariation zwischen der Nominalmode bei 165 GHz und den azimuthalen Nachbarmoden bei 162.75 und 167.2 GHz als auch eine kontinuierliche Frequenzvariation um bis zu 70 MHz innerhalb der Bandbreite der Nominalmode wurde demonstriert.

Die Verwendbarkeit der einzelnen Komponenten des Gyrotrons für einen Einsatz in einem 2 MW, CW Gyrotron wurde geprüft. In Übereinstimmung mit technischen Randbedingungen wurde eine geeignete Resonatormode ausgesucht. Ein geeigneter Kollektor für eine Strahleistung von 2.4 MW wurde vorgeschlagen und in Zusammenarbeit mit TED, Velizy, Frankreich wurde ein technischer Entwurf durchgeführt.

Im vorliegendem Bericht werden die erzielten Ergebnisse vorgestellt und diskutiert.

Contents

Executive Summary

Kurzfassung

1. Introduction	1
2. Experimental results	2-5
2.1 Parasitic low frequency oscillations	5 - 7
2.2 Results of RF measurements	7 - 9
2.3 Extension of the pulse length and high voltage performance of the gun	9 - 11
2.4 Mechanical stability of the coaxial insert	12 - 12
2.5 Losses at the coaxial insert	12 - 13
2.6 RF-stray radiation	13 - 15
2.7 Fast frequency tuning	15 - 17
3. A 2 MW, CW 170 GHz coaxial cavity gyrotron	18 - 18
3.1 Electron gun with coaxial insert	18 - 18
3.2 Cavity and operating mode	18 - 19
3.3 Quasi-optical output system	19 - 19
3.4 RF-output window	19 - 19
3.5 Collector	19 - 20
3.6 SC-magnet	20 - 20
3.7 RF-stray radiation and mirror box	20 - 20
3.8 Integration of the tube	20 - 22
4. Summary and Conclusions	22 - 22
Acknowledgments	22 -23
References	23 - 23
Publications in 2001 related to the task	23 - 24
Design tools at FZK	24 - 24

ITER ECRF ADVANCED SOURCE DEVELOPMENT

- Coaxial Cavity Gyrotron -

ITER task: G 52 TT 22 EU (TWO-ADV/SOR)

- final report, November 2001 -

B. Piosczyk, A. Arnold⁺, H. Budig, G. Dammertz, O. Drumm⁺, M. Kuntze and
M. Thumm⁺

Forschungszentrum Karlsruhe (FZK), Association EURATOM-FZK, Institut für Hochleistungsimpuls- und
Mikrowellentechnik (IHM), D-76021 Karlsruhe

⁺ also Universität Karlsruhe, Institut für Höchstfrequenztechnik und Elektronik

1. Introduction

The final goal of the development work, supported under the above mentioned ITER task, is to provide a basis for manufacturing of a 2 MW, 170 GHz coaxial cavity gyrotron for operation at long pulses up to CW as needed for ITER. Within this development work first the basic operating problems of a coaxial gyrotron have been studied as has been reported in the final report on "ITER ECRF COAXIAL GYROTRON AND WINDOW DEVELOPMENT (EU-T360), Part I: Coaxial Gyrotron Development ", February 1999.

To complete the data required for a technical realization of a coaxial gyrotron the following studies have been performed since then:

- investigation of stable operating conditions and of efficient microwave power generation
- study of the mechanism of low frequency (≤ 100 MHz) parasitic oscillations
- measurements of the mechanical stability of the coaxial insert under operating conditions
- measurements of losses at the coaxial insert and comparison with calculations
- investigation of the microwave stray radiation captured inside the gyrotron tube
- performance of fast frequency tuning (within 0.1 ms) by applying a bias voltage at the insert.
- investigation of the high voltage performance with increasing pulse lengths

Further on, a first draft integration of a coaxial gyrotron has been performed. Within this the suitability of the single components for a 2 MW, CW 170 GHz coaxial gyrotron has been investigated and the basic parameters and requirements have been specified. A possible operating mode which fulfills the technical restrictions has been selected.

In this final report first the recent (since the last report) experimental results are given and then the tube integration is presented with a discussion of the components.

2. Experimental results

The investigations have been performed with a gyrotron operated in the $TE_{31,17}$ mode at 165 GHz as already described in the last report in 1999. The schematic layout of the gyrotron is shown in Fig. 1. In difference to the previously used experimental set-up the main components as the electron gun, the cavity and the mirrors of the RF-output system have been newly designed and fabricated.

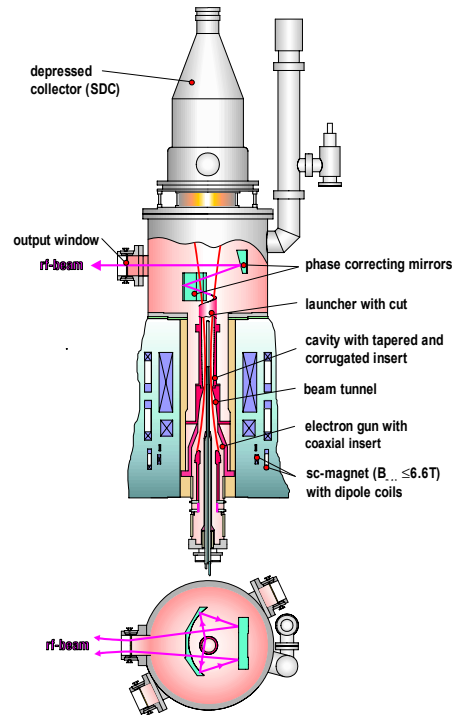


Fig.1: Schematic layout of a 165 GHz coaxial cavity gyrotron.

As electron gun a coaxial magnetron injection gun (CMIG) is used [1]. In the CMIG gun the electron beam is accelerated towards the anode as in guns of conventional gyrotrons and not towards the coaxial insert as in the previously used inverse magnetron injection gun (IMIG) [2]. The coaxial insert is supported from the bottom of the gun and is in total approximately 1 m long. The insert can be aligned under operating conditions with high accuracy (better than ± 0.05 mm) with respect to the electron beam by using the dipole coils. The cooling of the insert is provided by a water flow of about 10 l/min which is sufficient even for CW operation. The gun has been optimized for the following (nominal) parameters: beam current $I_b = 50$ A, cathode voltage $U_c = 90$ kV, magnetic field $B_{cav} = 6.65$ T, electron beam radius $R_b = 9.41$ mm and velocity ratio $\alpha = 1.4$. The performance of the electron beam in particular the velocity ratio α and the type of the electron flow near the cathode depend sensitively on the magnetic field distribution in the gun region which is determined by ratio of the currents in the two gun coils. Best operating conditions of the gyrotron has been observed

with an intermediate (between non laminar and quasi laminar) type of electron flow. A detailed discussion of the design and performance of the gun is given in [1].

The geometry of the cavity is shown in Fig. 2. The coaxial insert is longitudinally corrugated and tapered with an angle of -1 degree. The cavity has a quality factor of 2000 (cold) and about 2400 (self consistent). It has been optimized for an RF output power of about 1.5 MW for the nominal beam parameters and taking into account 10 % internal RF losses. The Ohmic losses at the outer cavity wall are calculated to be 0.54 kW/cm² (ideal copper) for an RF power of 1 MW. The calculated peak wall loading at the insert is only about 5 % of this value. The start-up behavior shown in Fig. 3 has been calculated with a self consistent, time dependent multimode code [3] assuming a relative transverse velocity spread $\delta\beta_{\perp rms} = 6\%$. The following modes have been considered as competitors: TE_{-30,17}, TE_{-32,17}, TE_{-33,17}, TE_{+29,17}, TE_{+29,18} and TE_{+28,18}.

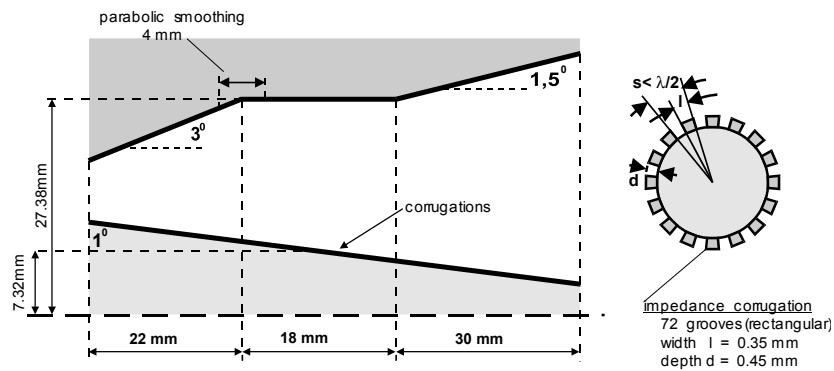


Fig. 2: Geometry of the TE_{31,17}, 165 GHz cavity.

The quasi-optical RF-output system consists of a smooth launcher with a single cut and of two mirrors - one quasi elliptical and one non-quadratic phase correcting mirror. The TE_{31,17} cavity mode is directly converted into a paraxial output beam with approximately a Gaussian power distribution in the window plane. The mirrors have been optimized for minimum diffraction losses inside the tube [4].

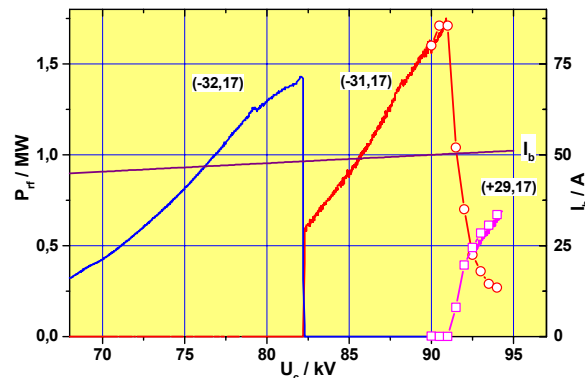


Fig. 3: The calculated RF-power generated in the cavity and the beam current in dependence of U_c . Start up behavior, U_c increases.

A disc of 100 mm diameter and a thickness of $13\lambda/2$ at 165 GHz either out of fused silica or out of BN (suitable for longer pulses) has been used as RF-output window.

The collector is insulated with respect to the tube body and in addition, the body is insulated from the ground (see Fig. 1) allowing operation in depressed mode either by positive biasing of the body and the insert or by negative biasing of the collector with respect to the ground.

The results presented in this paper have been achieved in three experimental campaigns, (1st: February - April 2000, 2nd: May -September 2001 and 3rd: October -November 2001). The first campaign ended accidentally due to a window failure which occurred during RF-operation. The gyrotron has been heavily polluted and had to be completely rebuilt. The cathode has been remachined. An unused emitter ring ordered for the first construction of the gun about 2 years ago was installed. All other components such as beam tunnel, cavity, launcher, RF output system and collector have been cleaned and baked out and used to restore the gyrotron. Thus for the second experimental campaign the tube has been rebuilt as it existed before the accident. The extension of the pulse length at the nominal parameters remained as a last experimental goal within the task. During high voltage conditioning a type of Penning discharge accompanied by a high current to the coaxial insert occurred inside the gun and limited the achievable pulse length. Unfortunately, since during the conditioning procedure the safety system for controlling the current to the insert was not in operation, the insert was overheated and a leak appeared which partly polluted the cathode. The insert had to be replaced and a lengthy conditioning of the tube became necessary to restore approximately the experimental operating conditions (3rd experimental campaign) before measurements with extended pulse length could start again.

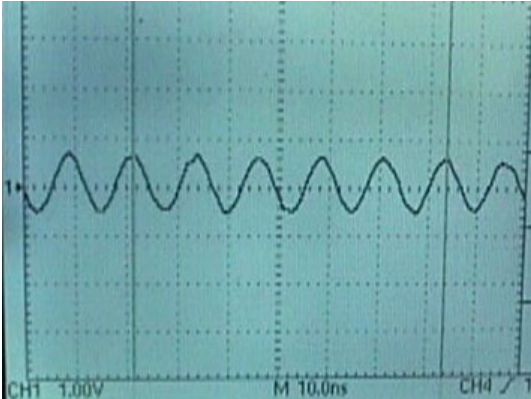
Results achieved in the three experimental periods are described in the following sections. First, observations in connection with parasitic low frequency oscillations, which occurred at the beginning of the first two experimental campaigns and which caused some difficulties in operation, are described. The origin of these oscillations has been studied and finally the oscillations have been successfully suppressed. Then results of microwave generation are given. Further experimental results concerning specific problems of the coaxial gyrotron as mechanical vibrations and losses at the coaxial insert, microwave diffraction losses and captured stray radiation are summarized. In addition, fast frequency tuning performed by applying a bias voltage to the coaxial insert has been demonstrated. The obtained results are described. The problems in achieving reliable high voltage performance at

an extended pulse length are due to the occurrence of a Penning type discharge inside the gun. The experimental observations are described and results of numerical analysis are discussed.

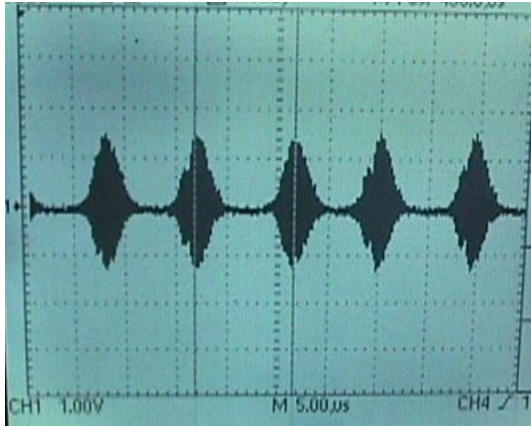
2.1 Parasitic low frequency oscillations

Parasitic low frequency oscillations in the frequency range below 100 MHz have been observed in various gyrotrons [5,6]. Such oscillations may cause severe problems, especially by disturbing the diagnostic system, and by deteriorating the quality of the electron beam.

At the beginning of the first two experimental campaigns such parasitic oscillations occurred. The frequency of these oscillations was either around 21, or 78 and 80 MHz. In all the cases the observed frequencies were practically independent of the operating parameters such as beam voltage, beam current and magnetic field. The radiation could easily be detected throughout the whole experimental area with a simple wire antenna and a fast oscilloscope. In addition, the oscillations have been observed as noise on diagnostic signals. An example of such parasitic oscillations with $f_{par} \approx 80$ MHz is shown in the Figs. 4a,b. The amplitude of the oscillations in the given case is modulated with about 100 kHz (Fig. 4b).



(a)



(b)

Fig. 4: Signal of parasitic low frequency oscillations. (a) 10 ns/div, (b) 5μs/div

These parasitic oscillations have been identified as occurring in the gun region. The cathode of an electron gun in a gyrotron can be considered as the end of an open coaxial resonator consisting of the HV-cable and the HV-supply on the opposite end. The resonance characteristic of this "cathode resonator" has been measured at low RF-power level for the used experimental setup and is shown in Fig. 5. The measured resonance frequencies agree reasonably well with the observed frequencies of the parasitic oscillations (indicated in Fig. 5). The mechanism of generation of the parasitic oscillations is assumed to be similar to the mechanism of a reflex klystron with electrons reflected at the magnetic mirror and with the cathode-anode region as resonator. The reflected and trapped electrons are therefore the driving force for generation of these parasitic oscillations. Thus these can be suppressed either by reducing the amount of reflected electrons, or by increasing the starting current due to reduction of the quality factor by damping the "cathode resonator".

In the experiments both methods have been applied successfully. In the first experimental period the parasitic oscillations were completely suppressed by redesigning the anode and a corresponding reduction of the α -value from about 1.6 to 1.4. The reduction of α resulted in a decrease of the amount of reflected electrons and thus stable operation of the gyrotron without parasitic oscillations became possible up to beam currents of 84 A.

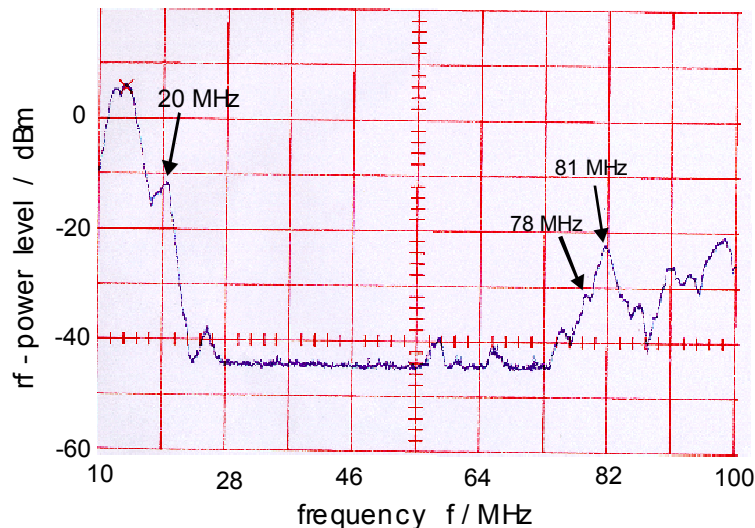


Fig. 5: The resonance characteristic of the gyrotron with electron gun connected via the high voltage cable with the power supply.

As already mentioned, for the second experimental period the gyrotron was brought into the same state as it was before the window failure. However, unlike the experimental behavior before the failure, parasitic oscillations were observed at beam currents above approximately 40 A. The frequencies of the parasites were the same as those observed at the beginning of the first experimental period. Simultaneously with the occurrence of parasitic oscillations, the current to the insert I_{ins} frequently increased suddenly from the values below 10 mA up to

above 1 A. The increase of I_{ins} has to be related with a strong rise of the radial beam width, since under normal conditions the smallest clearance between the electron beam and the insert inside the cavity is about 1.2 mm. The increase of the beam width is thought to be due to a beam instability related to trapped electrons oscillating between the magnetic mirror and the cathode.

The occurrence of parasitic oscillations in the second experimental period indicates that in this run the velocity spread has been larger than in the first experimental period. Mounting of some ferrite rings around the cables, connecting the anode and the insert either with the ground or with the high voltage supply, significantly improved the stability of operation and resulted in stable operation without parasitic oscillations up to beam currents of around 65 A.

2.2 Results of RF measurements

The RF-measurements were performed with a pulse length of typically 1 ms with a repetition rate of 1 Hz.

The frequency of the operating $TE_{31,17}$ mode was found to be very close to 165 GHz. Fig. 6 shows the RF-output power P_{out} and efficiency η_{out} as a function of the beam current I_b achieved in the first experimental period and the corresponding values of P_{out} obtained in the second period. For each value of the beam current the operating parameters U_c , B_{cav} , and the magnetic field distribution in the gun region have been optimized for maximum P_{out} . In the first experimental period RF output power as high as 2.2 MW was achieved at $I_b = 84$ A with an efficiency $\eta_{\text{out}} = 28$ %. A maximum output efficiency of 30 % (without depressed collector) was measured at the nominal power $P_{\text{out}} = 1.5$ MW. In the second experimental campaign measurements were performed up to a current of about 65 A. In that campaign the

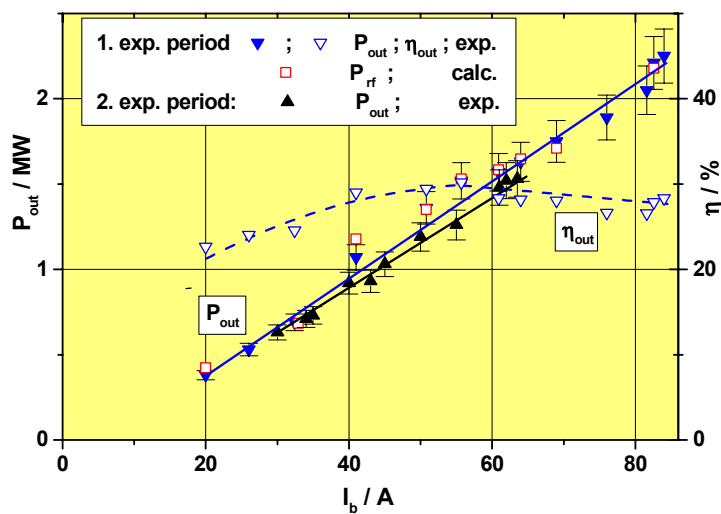


Fig. 6: Maximum RF-output power and efficiency as a function of the beam current, achieved in the first ($\blacktriangledown, \triangledown$) and second (\blacktriangle) experimental campaign and the calculated RF output power ().

maximum RF output power as a function of the beam current has been found to be smaller by few percent compared with the first campaign (Fig. 6). According to self consistent calculations this reduction can be explained by assuming a somewhat larger velocity spread, namely $\delta\beta_{\perp rms} = 8\%$ instead of 5% . The assumption of an increased velocity spread is consistent with the observation of parasitic oscillations in the second period, as described in the previous section. The calculated values given in Fig. 6 were obtained with the above mentioned self consistent, multi-mode code using the experimental parameters (first experimental period) as input. The velocity ratio has been obtained from trajectory calculations. For the velocity spread $\delta\beta_{\perp rms}$ a value of 5% has been assumed. The internal RF losses due to absorption and diffraction were assumed to be 10% . As is apparent from Fig. 6, there is a good agreement between the calculated values and the experimental results achieved in the first campaign. A similar agreement is obtained for the results of the second campaign with a spread $\delta\beta_{\perp rms} \cong 8\%$.

Operation with a single-stage depressed collector has been performed at an output power of 1.5 MW . As shown in Fig. 7 the efficiency has been increased from 30% up to 48% . No decrease of P_{out} has been observed if a negative retarding voltage up to about $U_{coll} = -34\text{ kV}$ was applied at the collector.

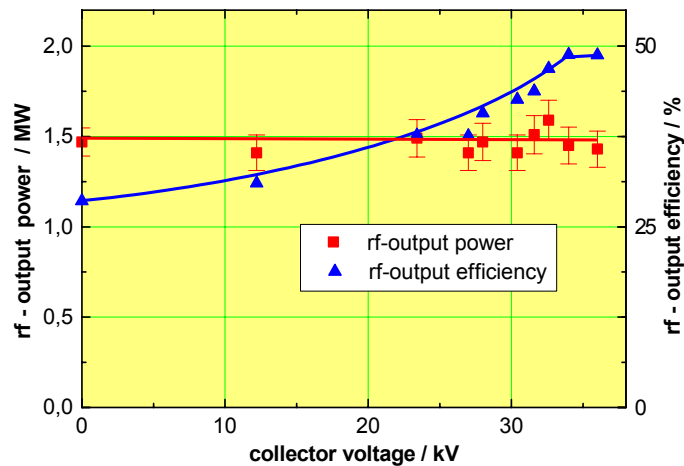


Fig. 7: RF-output power and efficiency as a function of the retarding collector voltage. All other parameters were kept constant.

The RF power distribution has been measured with an infrared camera at the window plane and outside the window at several distances. In Fig. 8a,b the measured distribution is compared with the results of calculations for a distance of 56.6 cm from the gyrotron axis. The displacement of the experimental RF power distribution from the axis of the output window (marked in the figures) is probably due to inaccuracy of measuring the position. Taking this into account there is good agreement between calculation and experiment. This confirms the reliability of the used design tools.

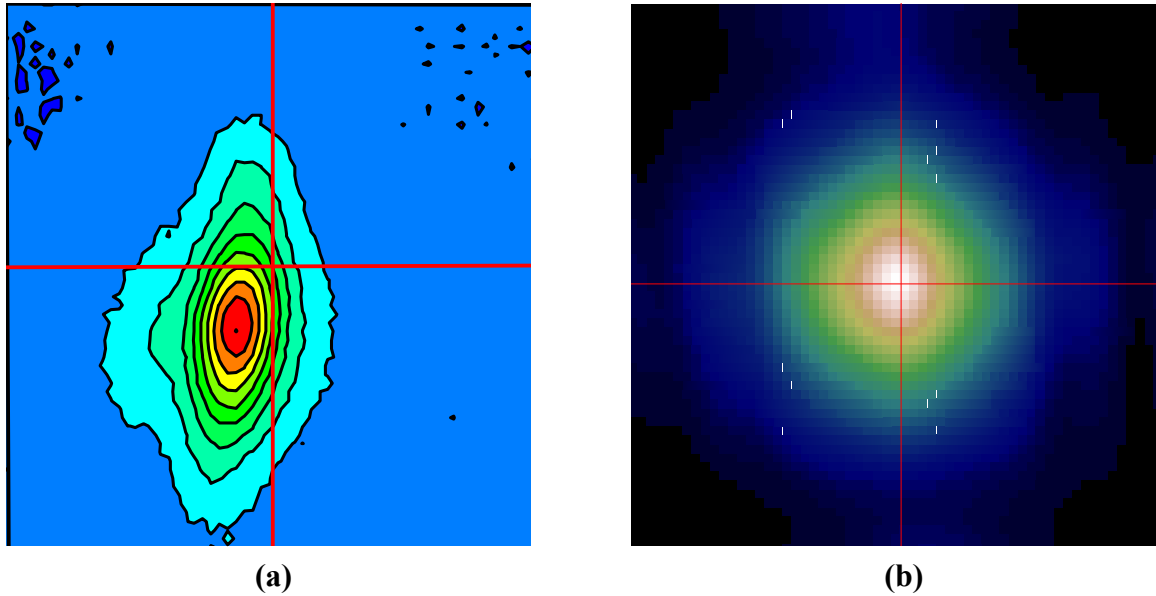


Fig. 8: The RF power distribution at a distance of 56.6 cm from the gyrotron axis, (a) measured and (b) calculated. Size of the shown section: $5 \times 5 \text{ cm}^2$.

2.3 Extension of the pulse length and high voltage performance of the gun

An extension of the pulse length has been performed around the nominal operating parameters ($I_b = 50 \text{ A}$, $U_b = 90 \text{ kV}$). After conditioning for a few days the achievable microwave pulse increased from a few ms at the beginning up to about 17 ms. The limitation of the microwave pulse was due to a sudden rise of the current I_{ins} to the insert causing a switching off of the body power supply which is used for applying the voltage to both the body and the insert. The pulse of the cathode voltage and the beam current remained up to 50 ms without a HV breakdown. The pressure increased during such a pulse from below 10^{-7} mbar up to about 5×10^{-6} mbar. The sudden rise of I_{ins} is thought to be due to built up of a discharge of Penning type.

The experimental observations are the following: A certain time τ_p after the beginning of the high voltage pulse I_{ins} increased suddenly to a large stationary value (up to several Amperes, depending on the external circuit). This has been observed independent from the flow of a beam current. However, a correlation between the vacuum conditions and the onset time τ_p has been noticed. In general, worse vacuum conditions resulted in a reduction of τ_p . When experiments for an extension of the pulse length have started first the current I_{ins} was not limited externally. Then during the conditioning the insert was heavily damaged due to an increase of I_{ins} to several Amperes. A small leak to the cooling water caused some pollution of the gun. The damaged insert had to be replaced before the experiments have been continued.

After replacing the insert the body current has been limited by a resistor of about $100 \text{ k}\Omega$ placed between the body power supply and the body and insert. The body voltage is applied to

both the insert and to the body. The Fig. 9 shows a typical trace with signals of the cathode voltage ($U_c \cong -60$ kV), the body voltage and of I_{ins} for a pulse with total length of 30 ms. The total accelerating voltage U_b is given by: $U_b = U_{body} + |U_c|$. The beam current I_b had a value of about 50 A. In the first part of the pulse from $\tau \cong 2$ ms up to $\tau_p \cong 19$ ms the applied body voltage is positive ($U_{body} \cong +28$ kV). During that time the $TE_{31,17}$ mode has been oscillating with an RF output power of about 1.1 MW. The value of I_{ins} saturates at about 25 mA. In the second part of the pulse starting with τ_p , I_{ins} increases suddenly to about 200 mA. Due to the

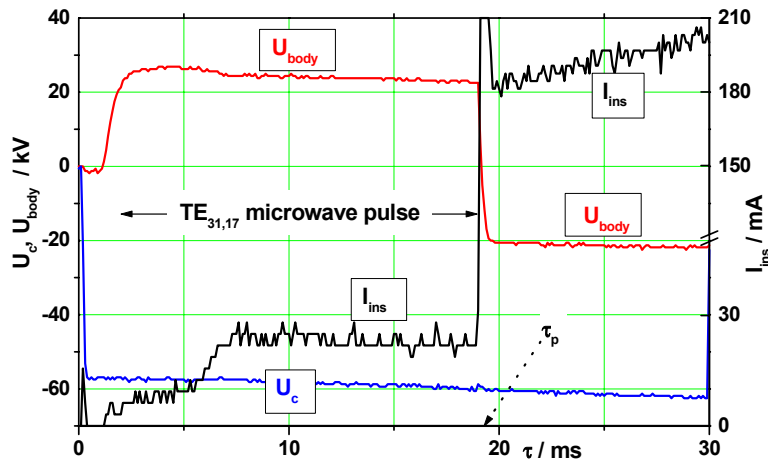


Fig. 9: A typical trace of U_c , U_{body} and of I_{ins} during a longer pulse. The length of the microwave pulse is indicated. The onset of the Penning discharge is at $\tau = \tau_p$.

rise of the current the power supply is switched off. The current through the 100 k Ω resistor is biasing the body to about -20 kV. The cathode voltage, however, remains constant over the whole pulse length. In separate measurements of the currents it has been found that in the most cases I_{ins} increased (as shown in Fig. 9) and only very seldom a rise of the current to the body has been observed. The Fig. 10 shows as an example the trace of the frequency signal as measured with a time frequency analyzer.

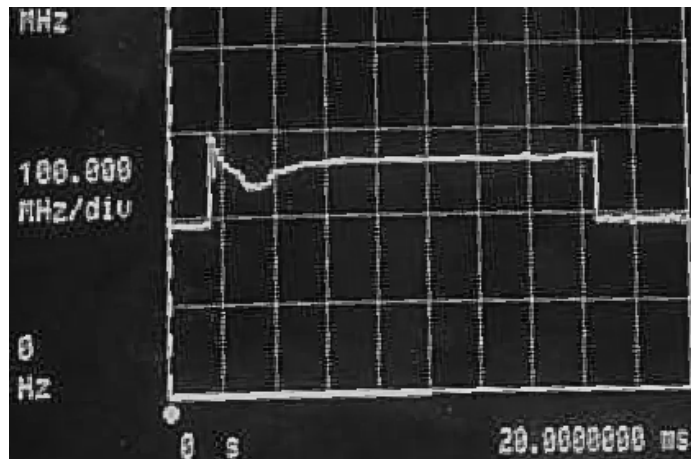


Fig. 10: A trace of the frequency signal of the generated microwave at 165 GHz. Frequency scale = 100 MHz/div, time scale = 5 ms/div.

The observed phenomena which limited the length of the microwave pulse are thought to be related to a Penning type discharge due to electrons trapped in the cylindrical symmetric arrangement of the crossed electric and magnetic fields inside the gun region. An extensive analysis of possible electron trajectories has been performed. Fig. 11 shows the lower ('technical') part of the electron gun. Two regions are indicated where electrons can be trapped and perform oscillations, a small region between the cathode and the anode and a large region located between the coaxial insert and the cathode. Electrons from this region may diffuse along the potential surfaces into the accelerating gap and are then accelerated along the magnetic flux surface towards the coaxial insert contributing to I_{ins} .

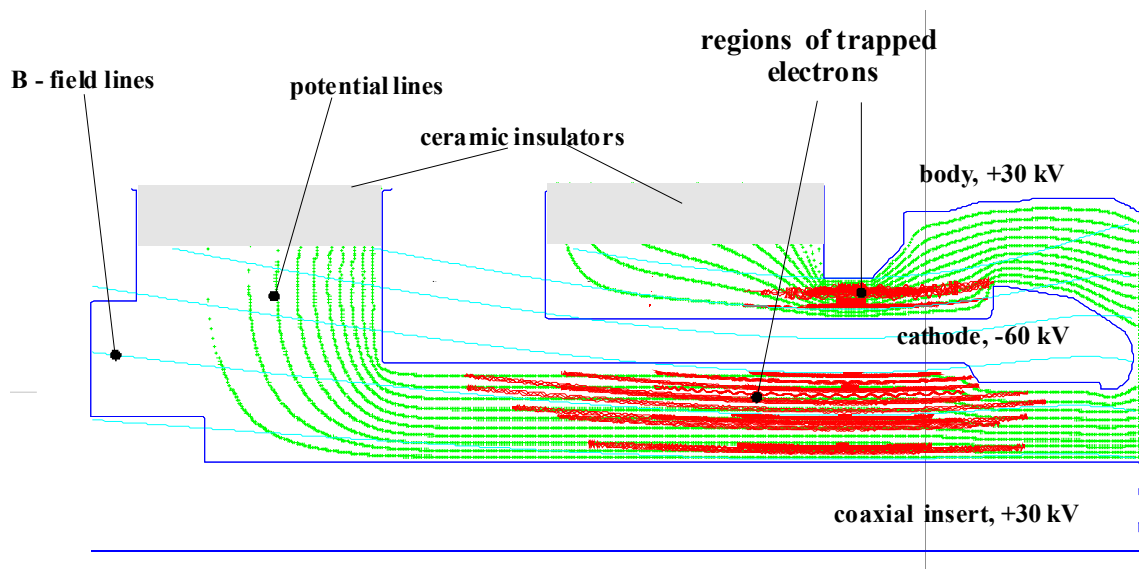


Fig. 11: The 'technical' part of the gun geometry with potential lines and magnetic fields. Two region with trapped electrons are indicated.

As a summary it can be said, that in the used gun the coaxial arrangement of the cylindrical insert and the cathode body together with the nearly paraxial distribution of the magnetic field forms a region with good conditions for trapping electrons. Trapped electrons performing oscillations are a necessary condition for the occurrence of a Penning discharge. In particular, the region between the cathode and the coaxial insert seems to responsible for the above described limitation of the pulse length due to the occurrence of the discharge. As a consequence, in designing a gun not only the shape of the electrodes have to be optimized. The whole gun geometry has to be designed in a way which prevents the occurrence of regions where electrons can be trapped. The design optimization has to take into account the real magnetic field distribution.

According to the results of numerical analysis a conventional gyrotron with a MIG gun geometry is less sensitive to the occurrence of such Penning discharges than a coaxial arrangement. However, in general such discharges may occur in MIG guns, too.

2.4 Mechanical stability of the coaxial insert

The mechanical stability of the coaxial insert is a crucial issue for stable long pulse and CW operation of coaxial gyrotrons. Therefore measurements of the mechanical vibrations of the insert have been performed under operating conditions. For this the electron beam was radially displaced inside the cavity with the help of the magnetic dipole coils until the beam touched the coaxial insert. The current to the insert I_{ins} depends on the amount of the radial displacement Δr_{beam} . The results are shown in Fig. 12. The measurements were performed in the following way. First, I_{ins} vs. Δr_{beam} was measured when the cooling water was turned off and the level of mechanical vibrations was very low (measured points in Fig. 12). When the water flow was turned on, the current I_{ins} varied within a certain range ΔI_{ins} (indicated in the figure) because of the vibration of the insert. From ΔI_{ins} , the maximum amplitude of the mechanical vibration is estimated to be within ± 0.03 mm. The main source of mechanical vibrations is the flow of the cooling water. The measured mechanical amplitude is sufficiently low to allow a stable long pulse operation. The value is in agreement with performed measurements of the vibration caused by mechanical knocking.

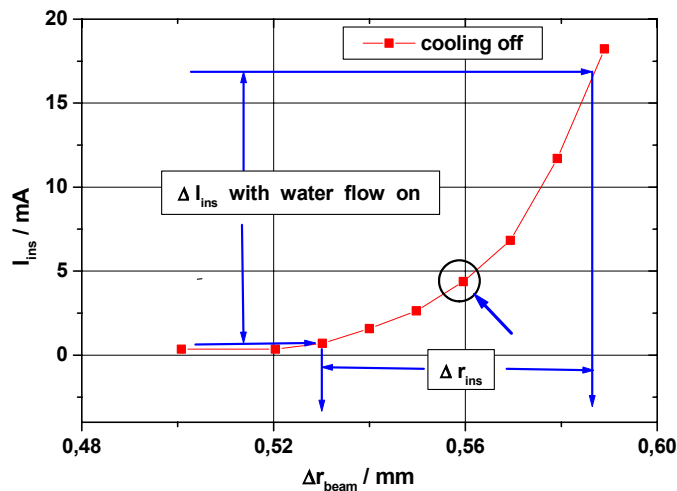


Fig. 12: Current to the insert as a function of the radial shift of the electron beam with cooling water off (■) and on (range of ΔI_{ins}).

2.5 Losses at the coaxial insert

Calorimetric measurements of the losses P_{ins} at the insert have been performed. Under stationary conditions a constant heat flow to the insert of about 70 W was observed which results from the radiation of the hot cathode to the cooled coaxial insert. The additional losses P_{ins} at the insert due to RF operation were measured as a function of the RF output power. Care was taken to ensure that during the measurements the gyrotron was oscillating in a single mode and that no beam instabilities with an increased value of I_{ins} occurred which would result in a rise of P_{ins} . The results are shown in Fig. 13. The calculated losses P_{calc} have been

obtained with a self consistent code assuming that the losses at a real surface are twice the losses of ideal copper [3,7]. The given range of $P_{\text{calc}}/P_{\text{out}}$ reflects the fact that the losses depend not only on P_{out} but also on other parameters such as U_c , I_b , B_{cav} etc.. The experimentally measured value of $P_{\text{ins}}/P_{\text{out}} \cong 10^{-3}$ is nearly twice as large as expected from calculations. The discrepancy may be caused due to a contribution related to I_{ins} as well as due to microwave dissipation of the captured stray radiation at the insert. Further experiments would be needed to separate the contributions from the two sources. However, the total losses at the insert are sufficiently small not to cause any problems even in CW operation with $P_{\text{out}} = 2$ MW.

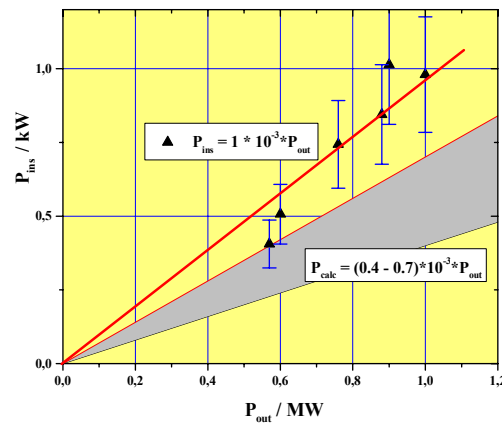


Fig. 13: Measured and calculated losses at the coaxial insert as a function of the RF output power for the $\text{TE}_{31,17}$ mode.

2.6 RF-stray radiation

The mirror box of the gyrotron is equipped with two relief windows of 100 mm diameter as shown in Fig. 14. It is seen that the arrangement of the two relief windows is not symmetric with respect to the mirrors and the RF output window. One of the relief windows has been equipped with a single fused silica disc (relative permittivity $\epsilon_r = 3.82$) and the other with a disc of BN ($\epsilon_r = 4.56$). The stray microwave power P_{relief} radiated out of the windows was measured with two bolometers. The bolometers consist of thin copper sheets covered with graphite, in order to enhance the absorption, two thermosensors, and a heater for calibration. They have a sensitivity limit of 0.1 Joule. The microwave absorption of the graphite layers has been measured to be between 10 and 18 % for normal incidence. The absorption increases to a value between about 17 and 30 % if the microwave power radiated through a window is assumed to be isotropic within a cone angle of 45 degrees around the normal direction, as is approximately the situation for the experimental setup. The uncertainty in knowing the absorption coefficient limits the accuracy of determining the absolute value of P_{relief} . It also limits the accuracy of the obtained total amount of the stray radiation P_{stray} caused mainly due

to diffraction losses at the launcher and the mirrors. All relative measurements, however, are accurate to within a few percent.

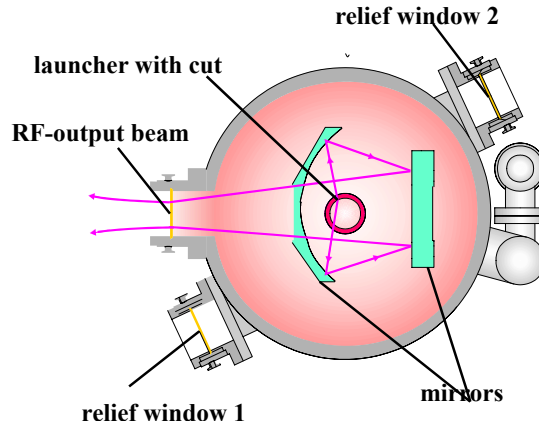


Fig.: 14 Arrangement of the two relief windows in the mirror box.

The relative value of the microwave power radiated through each of the two relief windows is shown in Fig. 15. The measurements have been performed at different pulse length τ_{pulse} in order to minimize the influence of the start up conditions at the beginning of a pulse. The results show that the power P_{relief} radiated through both relief windows is nearly the same. Since the geometrical position of the two relief windows is non symmetric (Fig. 14) these results suggest that the stray radiation P_{stray} captured inside the tube is distributed approximately uniformly inside the mirror box.

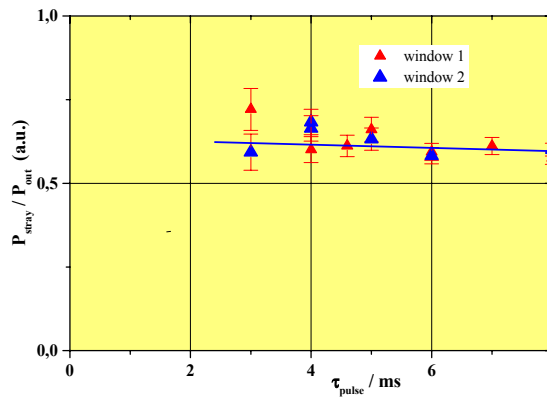


Fig. 15: The relative value of the microwave power radiated through the relief windows in dependence of pulse length.

The amount of the captured stray radiation P_{stray} which escapes through one relief window has been determined by measuring P_{relief} of one window both for the case when the second relief window was covered with a reflecting metal plate, and alternatively, with an absorbing material (piece of wood). Fig. 16 shows $P_{\text{relief}} / P_{\text{out}}$ of window 1 for different pulse lengths for the two cases either with a reflecting or with an absorbing plate at window 2. From the difference of $P_{\text{relief}} / P_{\text{out}}$ in both cases it can be concluded that in the investigated tube geometry with a mirror box made of stainless steel (diameter = 58 cm, height = 48 cm) and

with an insulating Al₂O₃ collector ceramic ring (diameter = 29 cm, length = 7 cm) only about 8 % of P_{stray} is radiated through a relief window: P_{relief} ≅ 0.08 × P_{stray}. Estimates suggest that a significant part (approximately 50 %) of P_{stray} is radiated through the ceramic insulation below the collector which thus acts as an efficient relief window and that about 30 % are absorbed in the walls of the mirror box.

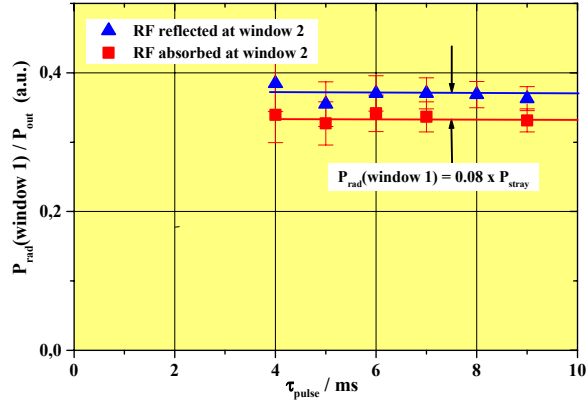


Fig. 16: The relative value of the microwave power radiated through one relief window in dependence of the pulse length as well with absorption and reflection at the other window.

As mentioned above, the absolute value of the power flow through the relief windows is known only with uncertainty of the absorption coefficient of the bolometers. With these uncertainty the total amount of diffraction losses is estimated to be about $(11 \pm 3) \%$ of the RF output power, $P_{\text{stray}} = (0.11 \pm 0.03) \times P_{\text{out}}$. This amount of the stray radiation is relatively large. Therefore, a redesign of the RF output system will be performed to reduce this value. However, the uniform distribution of the captured microwave radiation inside the mirror box keeps the technical problems related to dissipation of P_{stray} inside the tube under control, even for a 2 MW gyrotron.

2.7 Fast frequency tuning

The microwave frequency f of a gyrotron is determined by the resonance frequency of the cavity mode. In addition, the electron cyclotron frequency $f_c = \Omega_c / 2\pi = (1/2\pi) \times eB_{\text{cav}} / (m_0\gamma)$ with γ = relativistic mass factor, has to be close to f . Thus, f can be varied either stepwise by exciting different eigenmodes of the cavity or continuously within the bandwidth [6,8].

In the coaxial arrangement the energy of the electron beam E_b can be varied by applying a bias voltage U_{ins} at the coaxial insert. In addition to E_b the velocity ratio α also changes with U_{ins} . In the 165 GHz, TE_{31,17} cavity the beam energy depends on U_{ins} according to: $E_b = U_c + 0.82 \times U_{\text{ins}}$ [1]. Since the current to the insert is very small ($< 0.001 \times I_b$), a low power supply can be used.

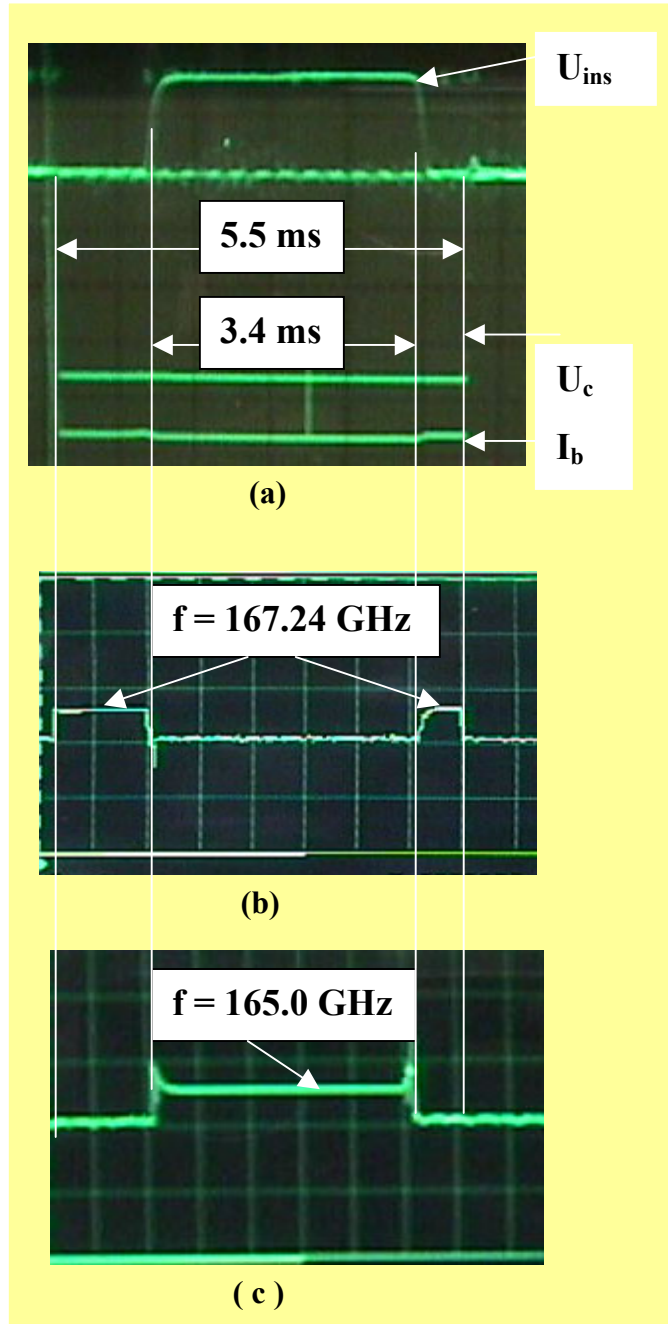


Fig. 17: Photography of the scope screen. (a) voltages U_c and U_{ins} and beam current I_b as applied for fast frequency tuning, (b) Frequency signal from the time frequency analyzer with $f = 167.24 \text{ GHz}$, (c) with $f = 165.0 \text{ GHz}$

By applying a variable bias voltage U_{ins} , fast stepwise frequency tuning between the nominal $TE_{31,17}$ mode (165.0 GHz) and its azimuthal neighbors, the $TE_{32,17}$ at 167.2 GHz and the $TE_{30,17}$ at 163.8 GHz as well as continuous tuning within the bandwidth of the $TE_{31,17}$ mode have been performed. Fig. 17a shows a characteristic scheme of the applied voltages U_c and U_{ins} which have been used for both step tuning and continuous frequency tuning. The pulse lengths used in the experiments are indicated in the figure. The beam current which also is shown depends practically only on U_c . The bias voltage U_{ins} (positive to ground) is applied with a delay with respect to the cathode voltage U_c (negative to ground). The employed power supply allowed a variation of the bias voltage within about 0.1 ms. If U_{ins} is varied, the

gyrotron continues to oscillate either in the currently excited mode (resulting in continuous frequency tuning), or the oscillation switches to a neighboring azimuthal mode, depending mainly on the values of B_{cav} , U_c and U_{ins} . This becomes clear by considering the start up scenario (Fig. 3) which shows the dependence of the excited modes on U_c . In Figs. 17b,c the signal of a time frequency analyzer is shown. At the beginning and at the end of the pulse, when U_{ins} is zero, the $TE_{32,17}$ mode is oscillating at 167.2 GHz (Fig. 17b). With the applied U_{ins} the gyrotron oscillates in the $TE_{31,17}$ mode at 165.0 GHz (Fig. 17c). The frequency switching between the modes by $\Delta f = 2.2$ GHz is done within about 0.1ms. The operating parameters had the following values: $B_{cav} = 6.64$ T, $I_b = 52$ A while U_c and U_{ins} were varied between 67 to 76 and 12.6 to 22 kV, respectively. The output power was about 1 MW at 165.0 GHz and almost 0.7 MW at 167.2 GHz. At 167.2 GHz the output window has a power reflection of about 20 %. A similar step frequency variation was also performed between the $TE_{31,17}$ mode at 165.0 GHz and the $TE_{30,17}$ mode at 162.75 GHz and even between the $TE_{32,17}$ mode at 167.2 GHz and the $TE_{30,17}$ mode at 162.75 GHz.

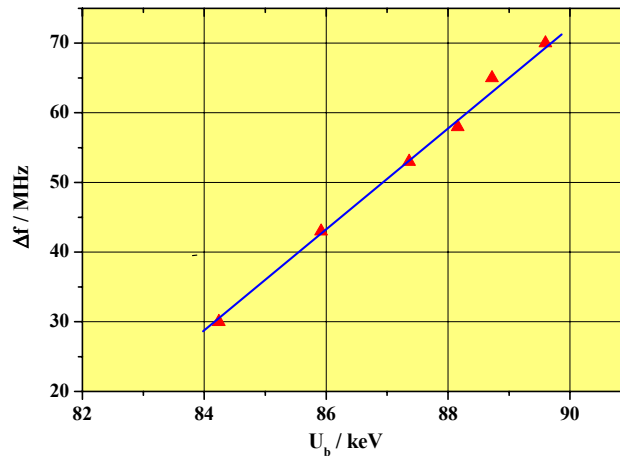


Fig. 18: Continuous frequency tuning in dependence of the bias voltage U_{ins} . $U_c = 81.2$ kV.

A continuous frequency variation has been performed within the bandwidth of the $TE_{31,17}$ mode at 165 GHz. The obtained frequency variation as a function of U_{ins} is shown in Fig. 18. A maximum frequency variation of 70 MHz has been achieved with $U_{ins} = 11$ kV. The measurements have been performed with $I_b = 51$ A and $U_c = 81.2$ kV. The microwave output power varied from 0.45 MW at $U_{ins} = 0$ up to about 1.1 MW at $U_{ins} = 11$ kV.

3. A 2 MW, CW 170 GHz coaxial cavity gyrotron

In the following first the status in the development of the single gyrotron components and their suitability a technical system is given and discussed. Some basic requirements are specified. Based on this a first integration has been performed and is presented.

3.1 Electron gun with coaxial insert

The electron gun used in the experiments [1] can be considered as a prototype for a 2 MW, CW gyrotron. The design has to be adjusted to the relevant magnetic field distribution and selected cavity mode. Based on the recent experience with extended pulse length care has to be given in designing the lower ('technical') part of the gun in order to avoid regions where electrons can be trapped and thus to eliminate the risk of occurring of a Penning discharge which may limit the HV performance. In experiments the generation of a stable electron beam with a current up to 84 A has been demonstrated. For an RF-output power of 2 MW not more than 75 A are expected to be needed. The corresponding emitter current density is about 4.4 A/cm^2 , higher than used in 1 MW tubes. However, this density should allow a lifetime in excess of 10000 h. The size of the gun is compatible with 220 mm diameter of the warm bore hole of the sc-magnet. The coaxial insert is supported from the bottom of the gun. The insert is cooled up to above the position of the cavity with about $10 \text{ lH}_2\text{O/min}$. According to numerical calculations the total RF-dissipation at the insert is expected to be between 0.5 kW and 1 kW with a peak power density below 0.1 kW/cm^2 (ideal copper).

3.2 Cavity and operating mode

The $\text{TE}_{31,17}$ -mode used in the 165 GHz gyrotron is not suitable to be used for a 2 MW at 170 GHz because of peak surface losses of 1.3 kW/cm^2 (ideal copper). A further disadvantage is the small radius ($R_{\text{ins}} = 7 \text{ mm}$) of the coaxial insert at 170 GHz. In this cavity, however, the $\text{TE}_{33,17}$ -mode at 169.5 GHz has been excited when step frequency operation has been done. Thus only minor modifications of the cavity size would be needed to adjust the cavity for 170 GHz in the $\text{TE}_{33,17}$ mode. However, according to calculations the peak wall loading is still slightly above the accepted technical limit of 1 kW/cm^2 , namely 1.1 kW/cm^2 (ideal copper) for an RF-output power of 2 MW (generated RF-power = 2.2 MW). In extensive calculations the $\text{TE}_{34,19}$ mode has been found as an acceptable candidate. At 2 MW output power the peak wall loading is 0.96 kW/cm^2 (ideal copper), the beam radius $R_b = 10 \text{ mm}$ and the radius of the insert $R_{\text{ins}} = 8 \text{ mm}$. The calculated electronic efficiency is 37 %. The loading at the coaxial insert has been calculated to be around 0.05 kW/cm^2 (ideal copper). If desired it would be

possible to verify the operation in the $TE_{34,19}$ mode with some small modifications on the existing set-up.

3.3 Quasi-optical output system

A q.o. RF-output system consisting of a Vlasov launcher, a quasi-elliptical mirror and a non-quadratic phase correcting mirror has been operated. Good agreement has been found between experiment and calculations. To generate a Gaussian distribution two phase correcting mirrors have to be used. A first design of such an RF-output system has been done. It has been used to perform a design of the integrated tube. A further optimization will be performed in order to reduce the diffraction losses.

3.4 RF-output window

A single disc CVD-diamond window can be used for transmission of 2 MW microwave power at 170 GHz. With a conservative value of the loss tangent, $\tan\delta \cong 4 \times 10^{-5}$ and a wall thickness of 1.66 mm the losses inside the CVD disc are calculated to be 1.06 kW. The resulting temperature difference between the center of the disc with a diameter of about 90 mm and the cooling rims is about 100 K. Since CVD diamond can be operated without risks to at least 300°C cooling with water at room temperature is still possible.

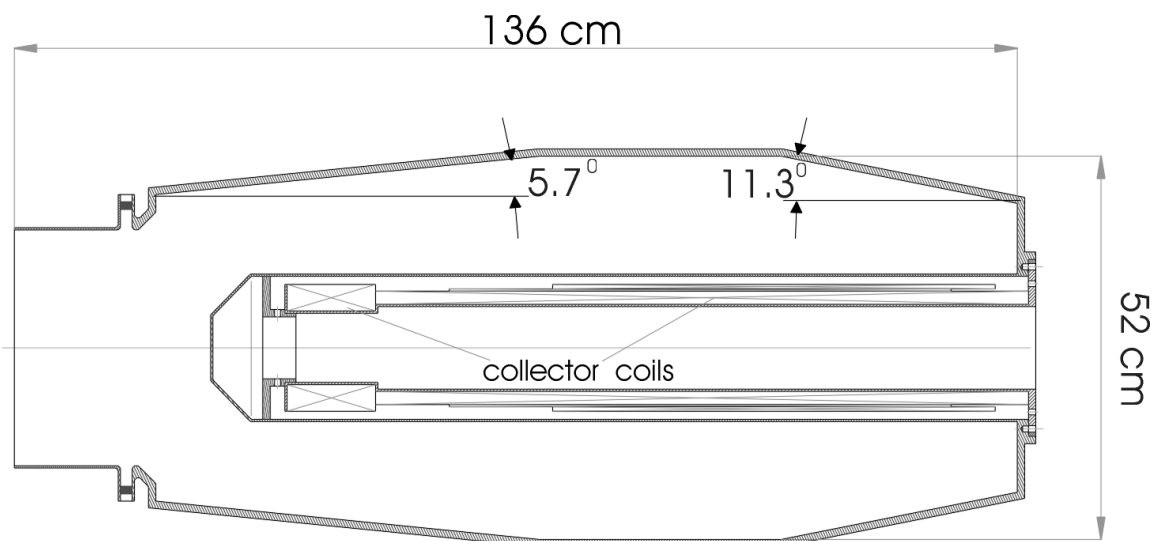


Fig. 19: Schematic layout of the collector.

3.5 Collector

At an RF-output power of 2 MW a dissipated beam power at the collector surface of up to 2.4 MW is expected if an output efficiency of $\geq 45\%$ is assumed as e.g. for the 1 MW, 140 GHz W7-X gyrotron. A new collector has been designed [9] and is shown in Fig. 19. By using a different arrangement of the collector sweeping coils a good power distribution along the collector surface is achieved. Thus the power loading along the collector surface stays

well within accepted technical limits and the size is approximately as for the 1 MW, 140 GHz tube. The feasibility for manufacturing has been examined and a technical design of this collector has been done by TED, Velizy, France.

3.6 SC-magnet

A SC-magnet with a warm bore hole of 220 mm diameter as used for the W-7X gyrotron is sufficient. A peak magnetic field of about 6.87 T is necessary. NbTi-technology should be applicable for fabrication of such a SC-magnet. However, detailed discussions with manufactures have to be done. In addition to the solenoidal coils a set of dipole coils similar as used in the experimental FZK-magnet is required in order to be able to perform the alignment of the insert and the tube under operating conditions.

3.7 RF-stray radiation and mirror box

The amount of stray radiation has been measured to be relatively large namely about 11% of the RF output power. Some reduction of this amount is expected by a further optimization of the RF output system. The fact that the microwave radiation captured inside the tube is uniformly distributed, reduces the problem related with removing the dissipated power in the body structure. However, an efficient cooling of all parts is necessary. A significant part of the stray radiation ($\approx 50\%$) is expected to radiated out of the box through the ceramic insulating ring of the collector.

3.8 Integration of the tube

A first integrated design based on the above given experimental results and on design calculations for a 170 GHz coaxial gyrotron with an RF output power of 2 MW, CW and taking into account the technical restrictions has been done and is shown in Fig. 20. The overall dimensions are comparable with the dimensions of a conventional 1 MW, CW gyrotron. The design of some components as beam tunnel and RF-output window can be taken from the design in the 1 MW, CW, 140 GHz gyrotron. A modular arrangement of certain groups of components is suggested. This allows an easy prove of the mechanical performance and of tolerances. The collector which is thought to be at ground potential is insulated from the body with an ceramic ring placed at the top of the mirror box. This has some advantages, namely (1) deceleration of the electrons occurs at relatively low magnetic field thus improving the efficiency of the energy recovery, (2) the electrical insulation of the cooling pipes can be done outside the gyrotron tube and (3) ceramic insulation ring of the collector acts as an efficient relief window. A disadvantage is the fact that the body and the mirror box are at high voltage and have to be insulated from the magnet.

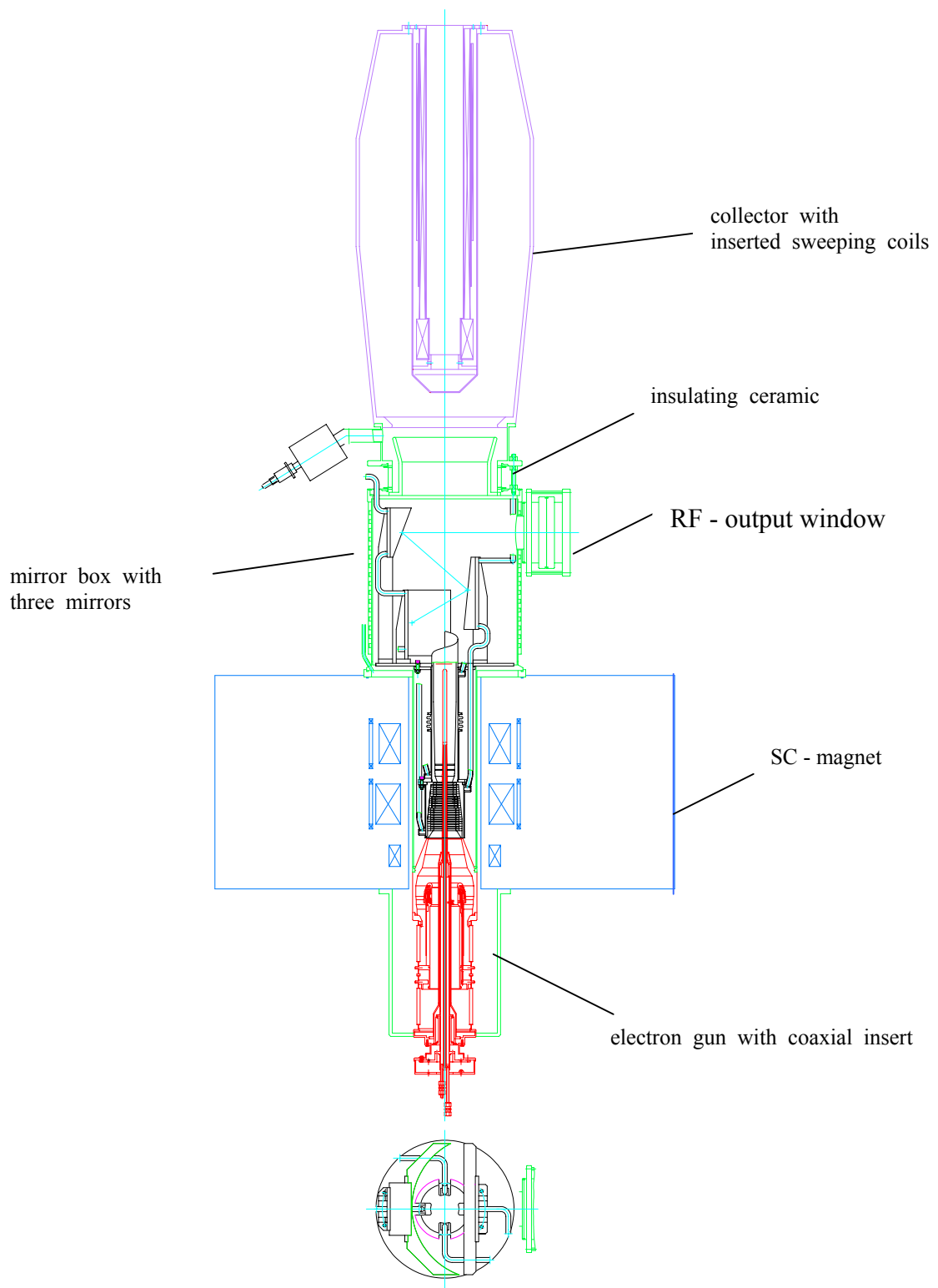


Fig. 20: Integrated 2 MW, CW 170 GHz coaxial gyrotron.

4. Summary and Conclusions

The obtained results prove the feasibility and provide the necessary data for manufacturing of a 2 MW, CW 170 GHz coaxial gyrotron as is of interest for application at ITER. In particular the following results have been achieved:

- A microwave output power up to 2.2 MW at 165 GHz has been generated stably in short pulse (ms) operation. In operation with a single-stage depressed collector the efficiency of 30 % has been increased up to 48 % at 1.5 MW (nominal output power).
- At nominal parameters a pulse length of 17 ms has been achieved after a few days of HV conditioning. The limitation of the pulse length is due to the occurrence of a discharge of Penning type in the gun region. The gun geometry in particular the cylindrical arrangement of the insert inside the cathode favors the trapping of electrons which is the reason for the observed Penning discharge. This effect has to be considered in future gun designs.
- The mechanical vibrations of the coaxial insert, which are mainly caused by the flow of the cooling water, have been found to be within ± 0.03 mm under operating conditions.
- The losses at the insert have been measured to be 0.1 % of the RF output power. This value which is about twice as large as the calculated RF losses is low enough not to cause any technical problems even in CW operation.
- The captured microwave stray radiation has been found to be approximately uniformly distributed inside the mirror box. The amount of the stray radiation is relatively high, namely around 11 %. The technical problems of removing the power at the walls of the box are reduced due to the uniform distribution of the stray radiation.
- Fast (~ 0.1 ms) frequency tuning has been performed by applying a bias voltage at the coaxial insert. Step frequency tuning by ± 2.2 GHz between the nominal mode and the nearest azimuthal neighbors and continuous frequency tuning by up to 70 MHz within the bandwidth have been demonstrated.

Acknowledgments

The part of the report on coaxial gyrotron development summarises the work assigned as an ITER TASK to the EU Home Team under an Agreement in the Engineering Design Activities for the International Thermonuclear Experimental Reactor ("ITER EDA Agreement"). The work was supported by the European Fusion Technology Program under the Project Nuclear Fusion of Forschungszentrum Karlsruhe. The authors acknowledge the contribution of H. Baumgärtner, P. Grundel, H. Kunkel, W. Leonhardt, D. Mallein, M. Schmid, J. Szczesny and R. Vincon of the gyrotron technical staff for the mechanical

design, the precise machining and the careful assembly of the tube, as well as for their assistance during the experiments.

References

- [1] B. Piosczyk, "A novel 4.5 MW electron gun for a coaxial gyrotron" IEEE Trans. Electron Devices, Dec. 2001, in press.
- [2] V.K. Lygin, B. Piosczyk, et al., "Inverse magnetron injection gun for a coaxial 1.5 MW, 140 GHz gyrotron", Int. J. Electronics, vol. 79,2, 1995, 227-235.
- [3] S. Kern, "Numerische Simulation der Gyrotron-Wechselwirkung in koaxialen Resonatoren", FZKA 5837, ISSN 0947-8620, Forschungszentrum Karlsruhe, Nov. 1996.
- [4] Michel, G., M. Kuntze, B. Piosczyk, M. Thumm: Considerations on multimode quasi-optical converters, Conf. Digest 24th Int. Conf. on Infrared and Millimeter Waves, Monterey, California, USA, 1999, PS-8.
- [5] V.E. Mjasnikov, M.V. Agapova, V.V. Alikae, et al. "Megawatt power level long-pulse 110 GHz and 140 GHz Gyrotrons", Proc. Int. Workshop on Strong Microwaves in Plasmas, August, 7-14, Nizhny Novgorod, Russia, 1996, 577-598.
- [6] K. Koppenburg et al., "Fast frequency step tunable high power gyrotron with hybrid magnet system", IEEE Trans. Electron Devices, vol.48, 2001, 101-107
- [7] O. Dumbrajs, B. Piosczyk, Ch. T. Iatrou, "Mode selection for a 2 MW, CW 170 GHz coaxial cavity gyrotron", 26th Inter. Conf. on Infrared and Millimeter Waves, Toulouse, F, September 10-14, 2001
- [8] Thumm, M; Arnold, A; Borie, E, O. Braz, G. Dammertz, O. Dumbrajs, K. Koppenburg, M. Kuntze, G. Michel, B. Piosczyk., "Frequency step-tunable (114-170 GHz) megawatt gyrotrons for plasma physics applications", Fusion eng. des., 53: 407-421 January 2001
- [9] B. Piosczyk , "A 2.2 MW, CW collector for a coaxial cavity gyrotron.", 26th Inter. Conf. on Infrared and Millimeter Waves, Toulouse, F, September 10-14, 2001.

Publications in 2001 related to the task:

- B. Piosczyk, "A novel 4.5 MW electron gun for a coaxial gyrotron" IEEE Trans. Electron Devices, Dec. 2001, Vol. 48, No. 12, 2938-44.
- B. Piosczyk, A. Arnold, E. Borie, G. Dammertz, O. Drumm, O. Dumbrajs, S. Illy, M. Kuntze, K. Koppenburg and M. Thumm, "Development of Advanced High Power Gyrotrons at Forschungszentrum Karlsruhe", Frequenz 55, 9-10 (2001), 242-246.
- Dumbrajs, O; Nikkola, P; Piosczyk, B., "On the negative-mass instability in gyrotrons", Int. J Electron, 88 (2): 215-224, February 2001
- Piosczyk, B.; Arnold, A.; Budig, H.; Dammertz, G.; Drumm, O.; Dumbrajs, O.; Kuntze, M.; Schmid, M.; Thumm, M., "Towards a 170 GHz, 2 MW, CW coaxial cavity gyrotron. Experimental results and design considerations."; 26th Inter. Conf. on Infrared and Millimeter Waves, Toulouse, F, September 10-14, 2001
- O. Dumbrajs, B. Piosczyk, Ch. T. Iatrou, "Mode selection for a 2 MW, CW 170 GHz coaxial cavity gyrotron", 26th Inter. Conf. on Infrared and Millimeter Waves, Toulouse, F, September 10-14, 2001

- Piosczyk, B.; Arnold, A.; Borie, E.; Dammertz, G.; Drumm, O.; Dumbrajs, O.; Illy, S.; Kuntze, M.; Koppenburg, K, Schmid, M.; Thumm, M., "Advanced high power gyrotrons for fusion applications."; 9th Triennial ITG-Conf.on Displays and Vacuum Electronics, Garmisch-Partenkirchen, May 2-3, 2001
- Piosczyk, B.; Arnold, A.; Borie, E.; Dammertz, G.; Drumm, O.; Dumbrajs, O.; Illy, S.; Kuntze, M.; Koppenburg, K, Schmid, M.; Thumm, M.; "Progress in the development of advanced high power gyrotrons."; 2nd IEEE Inter. Vacuum Electronics Conf., Noordwijk, NL, April 2-4, 2001
- C. T. Iatrou, K. Avramides, J.L. Vomvorides and B. Piosczyk, "Design Considerations of Powerful, Second-Cyclotron-Harmonic Coaxial-Cavity Gyrotrons"; 26th Inter. Conf. on Infrared and Millimeter Waves, Toulouse, F, September 10-14, 2001.

Design tools at FZK:

CAVITY:

At FZK a code system 'CAVITY' for simulation of the gyrotron interaction in coaxial cavities exists: CAVITY is a self-consistent, time dependent multimode code for calculation of interaction efficiency, start-up behavior, mode competition with up to 6 competing modes. It takes into account velocity spread of the electron beam. Different experimental results achieved for various operating conditions have been compared with the predictions of the numerical simulations. In general a good agreement has been obtained which strengthen the confidence to the results of numerical simulations.

A similar code with some additional features has been developed at the Technical University Helsinki.

OSSI:

The design of the q.o. RF-output system has been performed with a code system 'OSSI'. It allows to calculate the shape of the mirrors including non-quadratic phase corrected mirrors. A comparison of experimentally measured power distributions with design calculations showed a good agreement.

Codes for calculation of electron trajectories (BFCRAY, EGUN,EPOSR), magnetic field distributions (EFFI) are available at FZK.